A red/far-red light-responsive bi-stable toggle switch to control gene expression in mammalian cells

Published online 25 January 2013

Nucleic Acids Research, 2013, Vol. 41, No. 7 e77
doi:10.1093/nar/gkt002

A red/far-red light-responsive bi-stable toggle switch to control gene expression in mammalian cells

Konrad Müller[1], Raphael Engesser[2,3], Stéphanie Metzger[4,5], Simon Schulz[6], Michael M. Kämpf[1], Moritz Busacker[1], Thorsten Steinberg[6], Pascal Tomakidi[3,6], Martin Ehrbar[4,7], Ferenc Nagy[1,8], Jens Timmer[2,3,9,10,11], Matias D. Zubriggen[1] and Wilfried Weber[1,3,*]

[1]Faculty of Biology, University of Freiburg, Schänzlestrasse 1, 79104 Freiburg, Germany, [2]Department of Physics, University of Freiburg, Hermann-Herder-strasse. 3,79104 Freiburg, Germany, [3]BIOSS Centre for Biological Signalling Studies, University of Freiburg, Schänzlestrasse 18, 79104 Freiburg, Germany, [4]Department of Obstetrics, University Hospital Zurich, 8091 Zurich, Switzerland, [5]Institute of Bioengineering, Ecole Polytechnique Fédérale de Lausanne (EPFL), 1015 Lausanne, Switzerland, [6]Department of Oral Biotechnology, University Hospital of Freiburg, Hugstetterstrasse 55, 79106 Freiburg, Germany, [7]Zurich Center for Integrative Human Physiology, 8057 Zurich, Switzerland, [8]Biological Research Centre, Institute of Plant Biology, 6726 Szeged, Hungary, [9]Freiburg Centre for Biosystems Analysis (ZBSA), University of Freiburg, Habsburgerstrasse 49, 79104 Freiburg, Germany, [10]Freiburg Institute for Advanced Studies (FRIAS), University of Freiburg, Albertstrasse 19, 79104 Freiburg, Germany and [11]Freiburg Initiative in Systems Biology (FRISYS), University of Freiburg, Schänzlestrasse 1, 79104 Freiburg, Germany

Received August 1, 2012; Revised November 30, 2012; Accepted December 23, 2012

ABSTRACT

Growth and differentiation of multicellular systems is orchestrated by spatially restricted gene expression programs in specialized subpopulations. The targeted manipulation of such processes by synthetic tools with high-spatiotemporal resolution could, therefore, enable a deepened understanding of developmental processes and open new opportunities in tissue engineering. Here, we describe the first red/far-red light-triggered gene switch for mammalian cells for achieving gene expression control in time and space. We show that the system can reversibly be toggled between stable on- and off-states using short light pulses at 660 or 740 nm. Red light-induced gene expression was shown to correlate with the applied photon number and was compatible with different mammalian cell lines, including human primary cells. The light-induced expression kinetics were quantitatively analyzed by a mathematical model. We apply the system for the spatially controlled engineering of angiogenesis in chicken embryos. The system's performance combined with cell- and tissue-compatible regulating red light will enable unprecedented spatiotemporally controlled molecular interventions in mammalian cells, tissues and organisms.

INTRODUCTION

Inducible expression systems to control transgene activity represent a cornerstone technology in mammalian cell technology and synthetic biology. In contrast to chemically inducible systems that suffer from inherent drawbacks like complex pharmacokinetics of the inducer molecule (1), light at a cell-compatible wavelength represents a precisely adjustable stimulus for controlling gene expression at a high spatiotemporal resolution. In line with these advantages, synthetic optogenetic systems have been developed to control cellular signaling processes in bacteria, yeast and mammalian cells [reviewed in (2)]. For light-inducible gene expression in mammalian cells, blue light-responsive systems have been reported that are based on light-oxygen-voltage domains (2,3) or on the channel protein melanopsin (4). However, no light-inducible expression system for mammalian cells has been reported that is responsive to red light. The availability of such a system would be highly beneficial to

*To whom correspondence should be addressed. Tel: +49 761 203 97654; Fax: +49 761 203 2601; Email: wilfried.weber@biologie.uni-freiburg.de

mammalian cell technology, synthetic biology and tissue engineering, as red light is less toxic to cells and can penetrate tissues more efficiently than blue light.

We aimed at constructing a tunable red light-responsive gene expression system with rapid ON and OFF kinetics and minimal background. For this purpose, we capitalized on the red light-induced interaction of the photoreceptor phytochrome B (PhyB) and the phytochrome-interacting factor 6 (PIF6) of *Arabidopsis thaliana* (5). PhyB is a chromoprotein that consists of two main domains. The N-terminal part autoligates its chromophore phytochromobilin and is the photosensory domain that interacts with PIF6. The C-terminal part serves regulatory functions. PhyB is synthesized as the biologically inactive P_R form. On absorption of a red photon (660 nm), the chromophore isomerizes, thereby triggering a conformational change of the protein into the biologically active P_{FR} form, which can interact with downstream signaling components like PIF6. When the P_{FR} form absorbs a far-red photon (740 nm), it reverts back into the inactive P_R form terminating the interaction. The PhyB–PIF interaction has been used to control gene expression (6) and light-induced protein splicing in yeast (7), to induce actin polymerization in *Escherichia coli* (8) and for plasma membrane recruitment in mammalian cells (9). Although these results suggest that the PhyB–PIF interaction can be used for various signaling processes by using synthetic fusion proteins, no PhyB-based transcription system for mammalian cells has been reported.

MATERIALS AND METHODS

DNA cloning

The expression vectors and the detailed cloning strategy are described in Table 1.

Purification of phycocyanobilin from *Spirulina*

Phycocyanobilin (PCB) (molecular mass 586.7 g/mol) was purified from *Spirulina* by a modified protocol of Kunkel *et al.* (14). Fifty grams of *Spirulina* powder (Golden Peanut) was boiled with 500 ml of methanol for 1–2 min. After cooling, the liquid was removed by filtration, and the extraction was repeated 6–8 times until the flow through remained colorless. From this point onwards, all glassware was wrapped in aluminum foil, and all steps were carried out under green low-light conditions to protect the free chromophore. PCB was subsequently cleaved from its chromophore by methanolysis. Therefore, the extracted *Spirulina* powder was boiled in 500 ml of methanol for 4 h, the liquid was cleared by filtration, concentrated in a rotary evaporator to 30 ml and mixed with 70 ml of diethyl ether and 100 ml of 1% (w/v) aqueous citric acid. PCB was extracted from the organic phase with 50 ml of 1% (w/v) aqueous sodium hydrogen carbonate. The sodium hydrogen carbonate phase was acidified with 10 ml of 1 M HCl for PCB protonation before extraction with 50 ml of chloroform. The extraction was repeated for the aqueous citric acid phase from the first extraction step. The PCB-containing organic phases were combined and evaporated *in vacuo*, dissolved in 1.5 ml of dimethyl sulfoxide (DMSO) and stored at −20°C. The PCB concentration was determined photometrically as described elsewhere (9) and was typically 10–25 mM. This is equivalent to a total recovery of 2.5–6.5% based on the α6β6 hexameric structure of phycocyanin (Mw 225 kDa), with each α-subunit attached to one and each β-subunit attached to two PCB molecules and a phycocyanin content of 15% in dried *Spirulina* (15,16). Alternatively, PCB can be obtained from Livchem, Frankfurt, Germany (cat.no. P14137).

Cell culture, transfection, light induction and reporter gene assays

Chinese hamster ovary cells (CHO-K1, ATCC CCL 61) were cultivated in HTS medium (Cell Culture Technologies) supplemented with 10% fetal bovine serum (FBS) (PAN, cat. no. P30-3602, batch no. P101003TC) and 2 mM L-glutamine (Sigma). The monkey fibroblast-like cell line COS-7 (ATCC CRL-1651) and mouse embryonic fibroblasts (MEF, ATCC CRL-2214) were maintained in Dulbecco's modified Eagle's medium (PAN, cat. no. P03-0710) supplemented with 10% FBS. The mouse embryonic fibroblast cell line NIH/3T3 (ATCC CRL-1658) was cultivated in Dulbecco's modified Eagle's medium with 10% newborn calf serum (PAN, cat. no. 0402-P100104, batch no. 100104N). Primary human umbilical vein endothelial cells (HUVEC, PromoCell) were cultivated in endothelial growth medium 2 with supplement mix (PromoCell). Except for HUVEC cultivation, all media were supplemented with 100 U/ml of penicillin and 0.1 mg/ml of streptomycin (PAN). CHO-K1, COS-7, MEF and NIH/3T3 cells were transfected using a polyethylenimine-based method (PEI, linear, MW: 25 kDa) (Polyscience). In brief, 1 M PEI solution in H_2O was adjusted to pH 7.0 with HCl, sterile filtered and stored at −80°C in aliquots. In all, 30 000–70 000 cells were seeded per well of a 24-well plate and cultivated overnight. Aliquots of 0.75 µg of DNA were diluted in 50 µl of OptiMEM (Invitrogen) and mixed with 2.5 µl of PEI solution in 50 µl of OptiMEM under vortexing (amounts scaled to one well). After 15 min incubation at room temperature, the precipitate was added to the cells. For other plate formats, the cell number and amount of reagents were scaled up according to the growth area. For CHO-K1 cells, the culture medium was replaced 5 h after the transfection, whereas the DNA–PEI complexes remained on the other cell lines overnight.

HUVEC was transfected using FuGENE-HD Transfection Reagent (Roche). In all, 40 000 cells were seeded per well of a 24-well plate and cultivated overnight. Two micrograms of DNA was diluted in 95 µl of OptiMEM, and 5 µl of FuGENE-HD was added. After incubation for 15 min at room temperature, the lipoplexes were added to the wells.

Unless indicated otherwise, cells were transfected with the red light-dependent transcription factor encoded on plasmid pKM022 and the secreted alkaline phosphatase (SEAP) (pKM006)-, human vascular endothelial growth factor ($hVEGF_{121}$) (pKM033)- or mCherry (pKM078)-encoding reporter plasmids at a ratio of transcription

Table 1. Expression vectors and oligonucleotides designed and used in this study

Plasmid	Description	Reference or source
pKM001	Vector encoding SEAP under the control of P_{Tet} harboring a 394-bp spacer between the heptameric tetO operator and the minimal promoter ($tetO_7$–394bp$P_{hCMVmin}$–SEAP–pA). $tetO_7$–394 bp–$P_{hCMVmin}$ was chemically synthesized (Supplementary Table S1) and ligated (AatII/EcoRI) into pMK82.	This work
pKM002	Vector encoding SEAP under the control of a modified P_{Tet} harboring a 394-bp spacer between the 13mer tetO operator and the minimal promoter ($tetO_{13}$–394 bp–$P_{hCMVmin}$–SEAP–pA). $tetO_{13}$–394 bp–$P_{hCMVmin}$ was chemically synthesized (Supplementary Table S1) and ligated (AatII/EcoRI) into pMK82.	This work
pKM003	Vector encoding SEAP under the control of a modified P_{Tet} harboring a 394-bp spacer between the 20mer tetO operator and the minimal promoter ($tetO_{20}$–394 bp–$P_{hCMVmin}$–SEAP–pA). $tetO_{13}$–394 bp–$P_{hCMVmin}$ was excised (EcoRV/EcoRI) from pKM002 and ligated (NruI/EcoRI) into pKM001.	This work
pKM004	Vector encoding SEAP under the control of a modified P_{Tet} ($tetO_{26}$–394 bp–$P_{hCMVmin}$–SEAP–pA). $tetO_{20}$–394 bp–$P_{hCMVmin}$ was excised (EcoRV/EcoRI) from pKM002 and ligated (NruI/EcoRI) into pKM002.	This work
pKM006	Vector encoding SEAP under the control of a modified P_{Tet} harboring a 422-bp spacer between the 13mer tetO operator and the minimal promoter ($tetO_{13}$–422 bp–$P_{hCMVmin}$–SEAP–pA). A 372-bp fragment was amplified from *CFP* using oligos oKM001: 5′-caagtacctgcaggCCCTGAAGTTCATCTGCACC-3′ and oKM003: caagtcgctagcTCTTGAAGTTGGCCTTGATGC, digested (SbfI/NheI) and ligated (SbfI/NheI) into pKM002.	This work
pKM010	Vector encoding SEAP under the control of a modified P_{Tet} harboring a 488-bp spacer between the 13mer tetO operator and the minimal promoter ($tetO_{13}$–488 bp–$P_{hCMVmin}$–SEAP–pA). A 438-bp fragment was amplified from *CFP* using oligos oKM002: 5′-caagtacctgcaggACGTAAACGGCCACAAGTTC-3′ and oKM003: 5′-caagtcgctagcTCTTGAAGTTGGCCTTGATGC-3′, digested (SbfI/NheI) and ligated (SbfI/NheI) into pKM002.	This work
pKM014	Vector encoding SEAP under the control of a modified P_{Tet} harboring a 618-bp spacer between the 13mer tetO operator and the minimal promoter ($tetO_{13}$–618 bp–$P_{hCMVmin}$–SEAP–pA). A 568-bp fragment was amplified from *CFP* using oligos oKM002: 5′-caagtacctgcaggACGTAAACGGCCACAAGTTC-3′ and oKM004: 5′-caagtcgctagcTCTTTGCTCAGCTTGGACTG-3′, digested (SbfI/NheI) and ligated (SbfI/NheI) into pKM002.	This work
pKM017	Vector encoding a P_{SV40}-driven PhyB(1–908)–VP16–NLS expression unit [P_{SV40}–PhyB(1–908)–VP16–NLS–pA]. VP16–NLS was amplified from pMK216 using oligos oKM007: 5′-atcagtgaattcGATAGTGCTGGTAGT-3′ and oKM006: 5′-atcagttctagatcacaccttccgctttttcttgggCCCACCGTACTCGTCAATTC-3′, digested (EcoRI/XbaI) and ligated (EcoRI/XbaI) into pMK216.	This work
pKM018	Vector encoding a P_{SV40}-driven PhyB(1–650)–VP16–NLS expression unit [P_{SV40}–PhyB(1–650)–VP16–NLS–pA]. VP16–NLS was excised (EcoRI/XbaI) from pKM017 and ligated (EcoRI/XbaI) into pMK233.	This work
pKM019	Bicistronic vector encoding PhyB(1–908)–VP16 and TetR–PIF6(1–100)-HA under control of P_{SV40} [P_{SV40}–PhyB(1–908)–VP16–$IRES_{PV}$–TetR–PIF6(1–100)–HA–pA]. $IRES_{PV}$ was excised (PstI/NotI) from pMK082, PhyB(1–908)–VP16 was excised (AatII/PstI) from pMK216 and both fragment were ligated (AatII/NotI) into pMK235.	This work
pKM020	Bicistronic vector encoding PhyB(1–908)–VP16–NLS and TetR–PIF6(1–100)–HA under control of P_{SV40} [P_{SV40}–PhyB(1–908)–VP16–NLS–$IRES_{PV}$–TetR–PIF6(1–100)–HA–pA]. P_{SV40}–PhyB(1–908)–VP16–NLS was excised (AatII/PstI) from pKM017 and ligated (AatII/PstI) into pKM019.	This work
pKM021	Bicistronic vector encoding PhyB(1–650)–VP16 and TetR–PIF6(1–100)–HA under control of P_{SV40} [P_{SV40}–PhyB(1–650)–VP16–$IRES_{PV}$–TetR–PIF6(1–100)–HA–pA]. $IRES_{PV}$ was excised (PstI/NotI) from pMK082, PhyB(1–650)–VP16 was excised (AatII/PstI) from pMK233 and both fragment were ligated (AatII/NotI) into pMK235.	This work
pKM022	Bicistronic vector encoding PhyB(1–650)–VP16–NLS and TetR–PIF6(1–100)–HA under control of P_{SV40} [P_{SV40}–PhyB(1–650)–VP16–NLS–$IRES_{PV}$–TetR–PIF6(1–100)–HA–pA]. P_{SV40}–PhyB(1–650)–VP16–NLS was excised (AatII/PstI) from pKM018 and ligated (AatII/PstI) into pKM021.	This work
pKM028	Vector encoding the destabilized EYFP variant d2EYFP under the control of a modified P_{Tet} ($tetO_{13}$–422 bp–$P_{hCMVmin}$–d2EYFP–pA). $tetO_{13}$–422 bp–$P_{hCMVmin}$ was excised (SspI/EcoRI) from pKM006 and ligated (SspI/EcoRI) into pLMK164.	This work
pKM033	Vector encoding $hVEGF_{121}$ under the control of a modified P_{Tet} ($tetO_{13}$–422 bp–$P_{hCMVmin}$–$hVEGF_{121}$–pA). $hVEGF_{121}$ was amplified using oligos oKM015: 5′-caagtcgaattcaccgCCATGAACTTTCTGCTGTCTTG-3′ and oKM016: 5′-ctgaacgcggccgcTCACCGCCTCGGCTTGTC-3′, digested (EcoRI/NotI) and ligated (EcoRI/NotI) into pKM028.	This work

(continued)

Table 1. Continued

Plasmid	Description	Reference or source
pKM078	Vector encoding mCherry under control of a modified P_{Tet} ($tetO_{13}$–422 bp–$P_{hCMVmin}$–mCherry–pA). mCherry was excised (BamHI/NotI) from pMK047 and ligated (BamHI/Not) into pKM028.	This work
pLMK164	Vector encoding the destabilized EYFP variant d2EYFP under the control of P_{Tet} (P_{Tet}–d2EYFP–pA). dEYFP was excised (EcoRI/NotI) from pd2EYFP (Clontech) and ligated (EcoRI/NotI) into pMF111.	This work
pMF111	Vector encoding a P_{Tet}-driven SEAP expression unit (P_{Tet}–SEAP–pA).	(10)
pMK047	Vector encoding a $P_{EF1\alpha}$-driven mCherry expression unit ($P_{EF1\alpha}$–mCherry–pA). mCherry was amplified using oligos oMK057: 5′-ccaccactagtccaccATGGTGAGCAAGGGCGAGGAGG-3′ and oMK58: 5′-ggtgtgcggccgctcatatgtcctgtgagggttgaattcCTTGTACAGCTCGTCCATGCCGCCG-3′, digested (SpeI/NotI) and ligated (SpeI/NotI) into pWW029.	This work
pMK082	Vector encoding SEAP under the control of P_{Tet} ($tetO_7$–394 bp–$P_{hCMVmin}$–SEAP–pA). SEAP was excised (EcoRI/NotI) from pMF111 and ligated (EcoRI/NotI) into pWW927.	This work
pMK216	Vector encoding a P_{SV40}-driven PhyB(1–908)–VP16 expression unit [P_{SV40}–PhyB(1–908)–VP16–pA]. PhyB(1–908) was amplified from pAL149 (9) using oligos oMK246: 5′-caccgcggccgcCCACCATGGTTTCCGGAGTCGGGGGTAG-3′ and oMK247: 5′-ggtggcgcgcGGCTGTACGCGGAACCAGCACTACCAGCACTACCAG-3′, digested (NotI/BssHII) and ligated (NotI/BssHII) into pSAM200.	This work
pMK233	Vector encoding a P_{SV40}-driven PhyB(1–650)-VP16 expression unit (P_{SV40}–PhyB(1–650)-VP16-pA) PhyB (1–650) was amplified from pAL149 (9) using oligos oMK246: 5′-caccgcggccgcCCACCATGGTTTCCGGAGTCGGGGGTAG-3′ and oMK280: 5′-tacagaattcACCTAACTCATCAATCCCCTGTTCCC-3′, digested (NotI/EcoRI) and ligated (NotI/EcoRI) into pMK216.	This work
pMK235	Vector encoding a P_{SV40}-driven TetR–PIF6(1–100)–HA expression unit [P_{SV40}–TetR–PIF6(1–100)–HA–pA]. PIF6(1–100)–HA was amplified from pAL175 (9) using oligos oMK281: 5′-ccacgcgcgctcgatagtgctggtagtgctggtagtgctggtATGATGTTCTTACCAACCGATTATTGTTGC-3′ and oMK282: 5′-tactaagctttaagcgtaatctggaacatcgtatgggtaGTCAACATGTTTATTGCTTTCCAACATGTTTG-3′, digested (BssHII/HindIII) and ligated (BssHII/HindIII) into pSAM200.	This work
pRSet	P_{T7}-driven bacterial expression vector.	Novagen
pSAM200	Constitutive TetR–VP16 expression vector (P_{SV40}–TetR–VP16–pA).	(11)
pWW029	Vector encoding the erythromycin repressor protein E under control of $P_{EF1\alpha}$ ($P_{EF1\alpha}$–E–pA)	(12)
pWW800	Vector encoding VP16 under control of P_{SV40} (P_{SV40}–VP16–pA).	(13)
pWW927	Vector encoding SEAP under the control of P_{Tet} ($tetO_7$–ETR_8–$P_{hCMVmin}$–biotinidase–pA).	Weber *et al.*, unpublished data.

CFP, cyan fluorescent protein; d2EYFP, destabilized enhanced yellow fluorescent protein with a half-life of 2 h; E, erythromycin repressor protein; ETR_8, operator sequence binding E; EYFP, enhanced yellow fluorescent protein; HA, human influenza hemagglutinin-derived epitope tag; $hVEGF_{121}$, 121 amino acids splice variant of human vascular endothelial growth factor; $IRES_{PV}$, polioviral internal ribosome entry site; NLS, nuclear localization signal from simian virus 40 large T antigen; pA, polyadenylation signal; $P_{EF1\alpha}$, human elongation factor 1α promoter; $P_{hCMVmin}$, minimal human cytomegalovirus immediate early promoter; PhyB, phytochrome B; PhyB(1–650), N-terminus of phytochrome B with amino acids 1–650; PhyB(1–908), N-terminus of phytochrome B with amino acids 1–908; PIF6, phytochrome-interacting factor 6; PIF6(1–100), N-terminus of phytochrome-interacting factor 6 with amino acids 1–100; P_{SV40}, simian virus 40 early promoter; P_{Tet}, tetracycline-responsive promoter; SEAP, human placental secreted alkaline phosphatase; tetO, operator sequence binding TetR; TetR, tetracycline repressor protein; VP16, *Herpes simplex* virus-derived transactivation domain; YFP, yellow fluorescent protein. Uppercase in oligos, annealing sequence; underlined sequence, restriction site.

factor construct:promoter construct = 2:1 (w:w). After 24 h, the medium was replaced with fresh medium supplemented with 15 μM PCB. All experimental procedures after the addition of PCB were carried out under green LED light (522 nm). After 1 h cultivation in the dark, the cells were illuminated with 660 nm (8 μmol $m^{-2} s^{-1}$ unless indicated) or with 740 nm (80 μmol $m^{-2} s^{-1}$) light from LED arrays. Light intensity was adjusted using neutral density filters (Schott) that were placed on top of the culture dishes. For space-controlled gene expression, a photomask was placed underneath the culture plate that was subsequently illuminated from the bottom with 660 nm light (0.5 μmol $m^{-2} s^{-1}$) for 1 h followed by incubation in the dark for 24 h before detection of mCherry expression.

For control experiments, tetracycline was added at a concentration of 3 μg ml^{-1} from a 3 mg ml^{-1} stock solution in ethanol. The reporter SEAP was quantified in the cell culture medium using a colorimetric assay as described elsewhere (17). Fluorescence images of 100-mm dishes were taken using a BZ-9000 system (Keyence) and subjected to a Gaussian blur filter for noise reduction. VEGF was quantified using a human VEGF- enzyme-linked immunosorbent assay kit (Peprotech).

RNA-isolation and quantitative real-time polymerase chain reaction analysis

After cultivation, cells were lysed with RLT buffer (Qiagen) and homogenized with QiaShredder columns according to manufacturer's instructions (Qiagen), followed by total RNA isolation using the RNeasy mini kit (Qiagen). RNA concentration and integrity was analyzed using an automated electrophoresis system (Experion,

BioRad). First-strand cDNA was synthesized from 500 ng of total RNA using the RevertAid First-strand cDNA Synthesis Kit (Thermo Scientific). Therefore, both the provided random hexamer and the oligo $(dT)_{18}$-primers were used. The RNA and the primers were first incubated at 65°C for 5 min and chilled on ice for at least 5 min. Thereafter, the reaction mixture was added according to the manufacture's protocol and incubated at 25°C for 5 min, followed by 60 min at 42°C. The reaction was terminated at 70°C for 5 min. The cDNA concentration was fluorescently detected in a microplate reader (Infinite M-200, Tecan) using the Quant-iT PicoGreen dsDNA Assay Kit (Invitrogen) according to the manufacturer's protocol, and the cDNA concentration was adjusted to 50 ng/µl for each polymerase chain reaction (PCR). Quantitative PCR (qPCR) analysis was performed with the CFX96 real-time PCR detection system (BioRad). Quantitative amplification detection was achieved using the SABiosciences qPCR SYBR Green Master Mix (SABiosciences, Qiagen). For normalization, the housekeeping genes ß-actin (ACTB) and glyceraldehyde 3-phosphate dehydrogenase (GAPDH) were used. The PCR was performed with commercially available primers from SABiosciences for Chinese hamster ACTB and Chinese hamster GAPDH (SABiosciences). For determination of relative gene expression of $hVEGF_{121}$, the cloning primers oKM015 and oKM016 were used. For each PCR reaction, both primers were added at a concentration of 0.4 nM. The standard temperature profile included an initial denaturation step for 10 min at 95°C. Data were collected after every cycle of 40 cycles of denaturation at 95°C for 15 s, followed by annealing and extension at 60°C for 60 s, with an adjusted heating ramp of 1°C s^{-1}.

Chicken chorio-allantoic-membrane assay

For studying light-inducible angiogenesis, CHO-K1 cells engineered for red light-inducible $hVEGF_{121}$ expression were incubated with PCB (15 µM) for 1 h in the dark, detached and embedded in polyethylene glycol (PEG) hydrogels. These were then placed on the chicken chorio-allantoic membrane (CAM) and illuminated with 660 or 740 nm light.

The PEG gels were synthesized by mixing 1 million CHO-K1 cells transgenic for pKM022 and pKM033 with 8-arm PEGs [8-PEG–$MMP_{sensitive}$–Lys and 8-PEG–Gln, final PEG concentration: 3% (w/v)] in 50 mM Tris buffer (pH 7.6) containing 50 mM $CaCl_2$ and 50 µM Lys–RGD. Gel formation (20 µl final gel volume in a microdome shape) was induced by Factor XIIIa-catalyzed cross-linking of the lysine and glutamine-functionalized PEG polymers via transglutaminase reaction (18).

Experiments on chicken embryos were conducted following the shell-free cultivation protocol (19). After 3 days of incubation at 37°C, Brown Leghorn eggs were opened, and their contents were carefully poured into plastic Petri dishes of 100 mm in diameter. The chicken embryos were further incubated for 6 days at 37°C in a humidified atmosphere. On embryonic day 9, the cell-containing PEG gels were placed on the surface of the CAM. After 2 days of further incubation under 660 nm (8 µmol m^{-2} s^{-1}) or 740 nm (80 µmol m^{-2} s^{-1}) light, the CAMs were examined by *in vivo* microscopy after injecting 100 µl of 2.5% fluorescein isothiocyanate (FITC)–Dextran (2000 kDa, Sigma) into the CAM vasculature. The vasculature was assessed by video microscopy for morphological changes in the vessel structure and capillary plexus.

RESULTS AND DISCUSSION

We designed the red light-inducible expression system based on the concept of split transcription factors (Figure 1a and b). For this aim, we fused the tetracycline repressor TetR (20) to the N-terminal half of PIF6 (amino acids 1–100) that was shown to be sufficient for selective binding to the P_{FR} form of PhyB (5,9). The photosensory N-terminal domain of PhyB (amino acids 1–650 or 1–908) was fused to the *Herpes simplex*-derived transactivation domain VP16 and optionally to a nuclear localization sequence. The split transcription factor components were expressed from a bicistronic expression vector (Figure 1a). The response construct was designed by fusing multiple (7, 13, 20, 26) repeats of the TetR-specific tetO operator to the minimal human cytomegalovirus immediate early promoter ($P_{hCMVmin}$) via spacers of different length (394, 422, 488 and 618 bp, Figure 1a). The natural PhyB chromophore phytochromobilin is not found in mammalian cells, but it can be substituted for PCB that is conveniently extracted from the cyanobacterium *Spirulina* and when added to the culture medium is autoligated to PhyB (9). On illumination with red light, $PhyB_{FR}$ interacts with PIF6, thereby reconstituting a functional transcription factor that binds tetO via the TetR motif and mediates RNA polymerase II-dependent transcription from $P_{hCMVmin}$ via the VP16 transactivation domain. On illumination with far-red light, the PIF6–PhyB interaction is dissociated, and gene expression remains silent (Figure 1b).

To determine the molecular configuration resulting in optimum induction characteristics, we evaluated red light-inducible gene expression profiles in CHO-K1 using human placental SEAP as reporter gene. For optimizing the transcription factor, we evaluated the impact of PhyB truncations (amino acids 1–650 or 1–908) and the presence or absence of a nuclear localization sequence (NLS). Comparison of SEAP production in red (660 nm) or far-red (740 nm) light revealed that the shorter PhyB variant in combination with an NLS resulted in superior induction characteristics (Figure 1c). For determining the optimum promoter configuration, we varied the number of tetO repeats (Figure 1d) and the spacer length separating tetO from $P_{hCMVmin}$. The maximum induction factor was observed for 13 tetO repeats and a spacer of 422 bp (Figure 1e) that were used throughout the subsequent experiments. Transfection of the red light-inducible expression system in different human-, mouse-, hamster- and monkey-derived cell lines or human primary cells resulted in up to 65-fold induction levels, suggesting a cross-species applicability of this expression control strategy (Figure 1f and Supplementary Figure S1). For biomedical applications, it is important to titrate gene

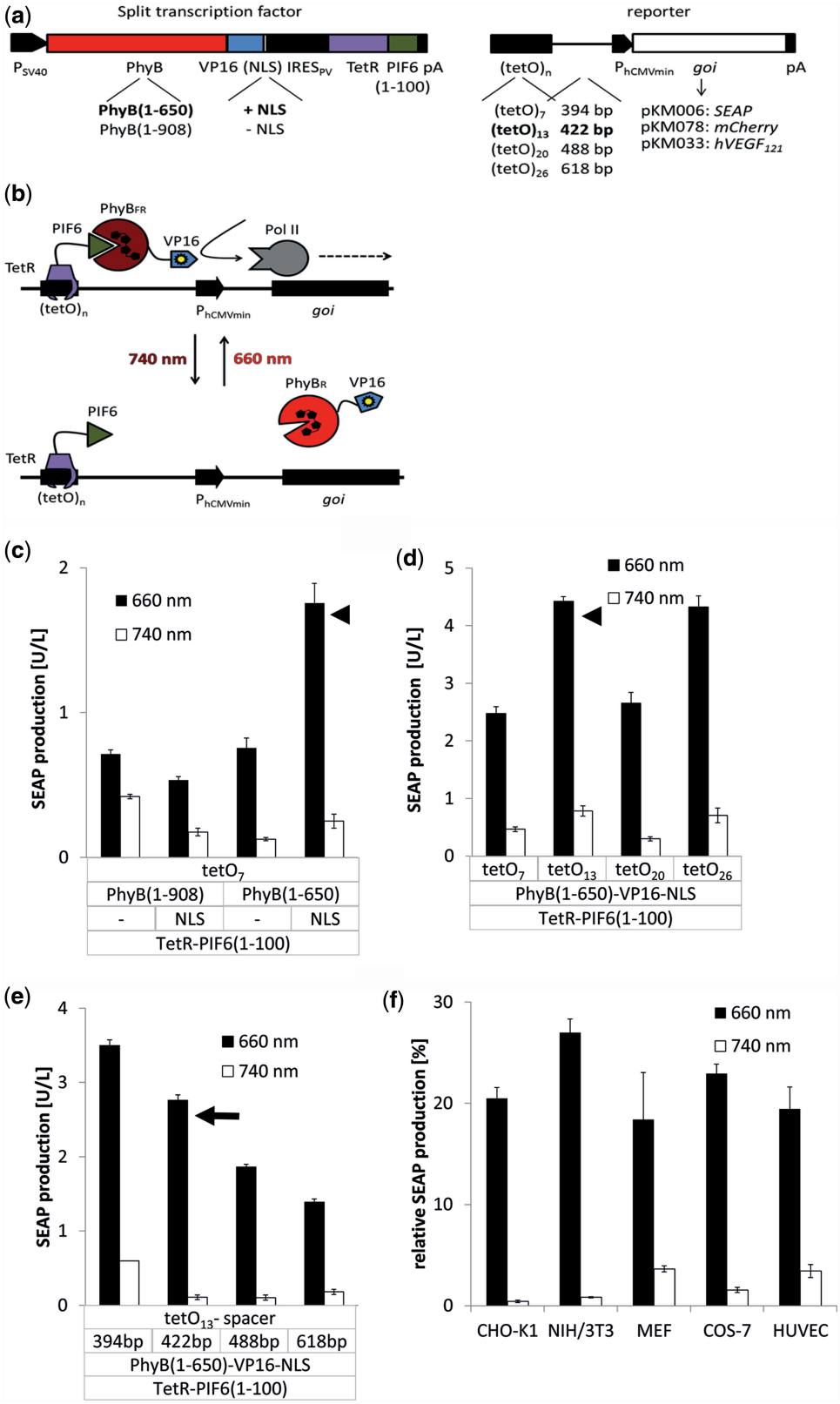

Figure 1. Design, optimization and validation of the red light-inducible transgene expression system. (**a**) Configuration of the red light-inducible expression system. The building blocks for the split transcription factor are encoded on a bicistronic expression vector under the control of the simian virus 40 promoter P_{SV40}. In the first cistron, the N-terminal fragments of PhyB (amino acids 1–650 or 1–908) are fused to VP16 and optionally to an NLS. In the second cistron, the N-terminal 100 amino acids of PIF6 are fused to the tetracycline repressor TetR. Translation of the second cistron is induced by a polioviral internal ribosome entry site, $IRES_{PV}$. The response vectors comprise multiple repeats of the TetR-specific operator tetO fused via spacers of different length to the minimal human cytomegalovirus immediate early promoter $P_{hCMVmin}$. This chimeric promoter was configured to

(continued)

expression into the therapeutic window. To characterize adjustable gene expression characteristics of our system, CHO-K1 cells were transfected with the optimized expression system and incubated either under increasing light intensity or in the presence of increasing PCB concentrations. SEAP production was shown to be adjustable by the photon number (Figure 2a) reaching full expression levels already at a dose as low as 80 nmol cm^{-2} as well as by the chromophore concentration (Figure 2b). By substituting PhyB(1–650)–VP16–NLS for VP16, we ensured that PCB itself has no effect on gene expression at the optimal concentration of 15 μM (Supplementary Figure S2).

A key advantage of using light as inducer is the high temporal precision by which it can be applied or removed from the biological system (21). To evaluate whether our system allows for light-triggered time-resolved gene expression, we introduced the system into CHO-K1 cells that were subsequently subjected to alternating cycles of 660 or 740 nm light for 24 h each. Repeated high expression levels under induced conditions and background levels under repressed conditions suggest full reversibility of transgene expression (Figure 2c). It is known that the P_{FR} form of PhyB is not only converted to P_R by far-red light but also that this process also takes place in the dark with slower kinetics (22). We characterized the impact of this dark reversion by inducing gene expression at 660 nm for increasing periods of time (0–24 h) before moving the cells to the dark. Illumination for only 3 h was shown to be sufficient to sustain transgene expression for another 21 h in the dark, indicating that spontaneous dark reversion does not have a significant impact on transgene expression (Figure 2d). These characteristics are reminiscent to a bi-stable toggle switch (23), where short stimuli are sufficient to switch the system from one stable state to the other, thus avoiding the prolonged application of the inducer while still having the opportunity to switch the system at any desired point in time.

Another major advantage of light over chemical inducers is the ability to spatially control gene expression. To characterize spatially restricted gene expression, we engineered CHO-K1 cells for red light-inducible expression of the fluorescent protein mCherry. Application of red light through a photomask to the cell monolayer and subsequent fluorescence imaging revealed an mCherry expression pattern that precisely reproduced the shape of the photomask, thus validating the system's suitability for space-resolved gene expression (Figure 2e).

To quantitatively understand the underlying processes in light-inducible gene expression, we developed a quantitative mathematical model that we parameterized by the experimental data. The model was based on ordinary differential equations describing the concentrations of the molecular components in a single cell. A detailed model derivation is described in Supplementary Information.

$$\frac{d[PCB](t)}{dt} = -k_{deg,PCB}[PCB] - k_{form,PPV}[PhyB{-}VP16]\frac{[PCB]}{K_{m,PCB}+[PCB]} \quad (1)$$

$$\frac{d[PPV](t)}{dt} = -k_{deg,PPV}[PPV] + k_{form,PPV}[PhyB{-}VP16]\frac{[PCB]}{K_{m,PCB}+[PCB]} \quad (2)$$

$$\frac{d[mRNA](t)}{dt} = -k_{deg,mRNA}[mRNA] + [GD]\left(k_{basal,mRNA}+k_{tc}\frac{k_{light}[PPV]}{K_{m,tc}+[PPV]}\right) \quad (3)$$

$$\frac{d[P_{pre}](t)}{dt} = -k_{out}[P_{pre}]+k_{tl,P_{pre}}[mRNA] \quad (4)$$

$$\frac{d[VEGF](t)}{dt} = -k_{deg,VEGF}[VEGF]+k_{tl,VEGF}[P_{pre}] \quad (5)$$

$$\frac{d[SEAP](t)}{dt} = -k_{deg,SEAP}[SEAP]+k_{tl,SEAP}[P_{pre}] \quad (6)$$

$$\frac{dGD(t)}{dt} = -k_{dilution}GD \quad (7)$$

$$\frac{dN(t)}{dt} = k_{growth}N \quad (8)$$

with $[PhyB{-}VP16] = PhyB{-}\mathrm{VP16}_{total_0}GD - [PPV]$

The mRNA production is described in Equation (3). The parameter $k_{basal,mRNA}$ represents the basal mRNA transcription rate which is independent of the

Figure 1. Continued
control expression of different genes of interest (goi): SEAP, secreted alkaline phosphatase; $hVEGF_{121}$, 121 amino acid splice variant of human vascular endothelial growth factor or the fluorescent protein mCherry. (**b**) Mode of function. Red light illumination converts PhyB into the FR form ($PhyB_{FR}$) and induces heterodimerization with PIF6 tethered via TetR to the $tetO_n$ operator site. The PhyB-fused VP16 domain recruits the transcription initiation complex and triggers activation of the minimal promoter $P_{hCMVmin}$. Absorption of a far-red photon (740 nm) converts PhyB into the R form ($PhyB_R$) and triggers dissociation from PIF6, thereby resulting in de-activation of the target promoter and transcriptional silence. (**c–e**) Optimization of the red light-inducible expression system in CHO-K1. The indicated configurations of the red light-inducible expression system were transfected into 70 000 CHO-K1 cells. After incubation for 24 h, medium containing 15 μM PCB was added. After 1 h incubation in the dark, the cells were exposed for 24 h to red (660 nm) or far-red (740 nm) light before quantification of the reporter gene SEAP. (c) Impact of PhyB variant (908 or 650 amino acids) and the absence or presence of an NLS. (d) Impact of the tetO copy number. (e) Impact of spacer length between the operator and the minimal promoter. Arrowheads mark the configurations that were optimized in the subsequent experiments. The configuration showing the best induction ratio (arrow) was used for the subsequent studies. (**f**) Characterization of red light-inducible gene expression in different mammalian cell lines. Plasmids pKM022 and pKM006 were transfected into CHO-K1, mouse fibroblasts (NIH/3T3, MEF), monkey fibroblasts (COS-7) and primary HUVEC. After 24 h, medium containing 15 μM PCB was added. The cells were subsequently incubated for 1 h in the dark, and further cultivated under 660 or 740 nm light for 24 h before quantification of SEAP production. To correct for different transfection efficiencies for the different cell lines, the expression data were normalized to SEAP expression levels under the control of the tetracycline-inducible expression system (vectors pSAM200 and pKM006, Table 1). Data are means of four independent experiments, and error bars indicate the standard deviation.

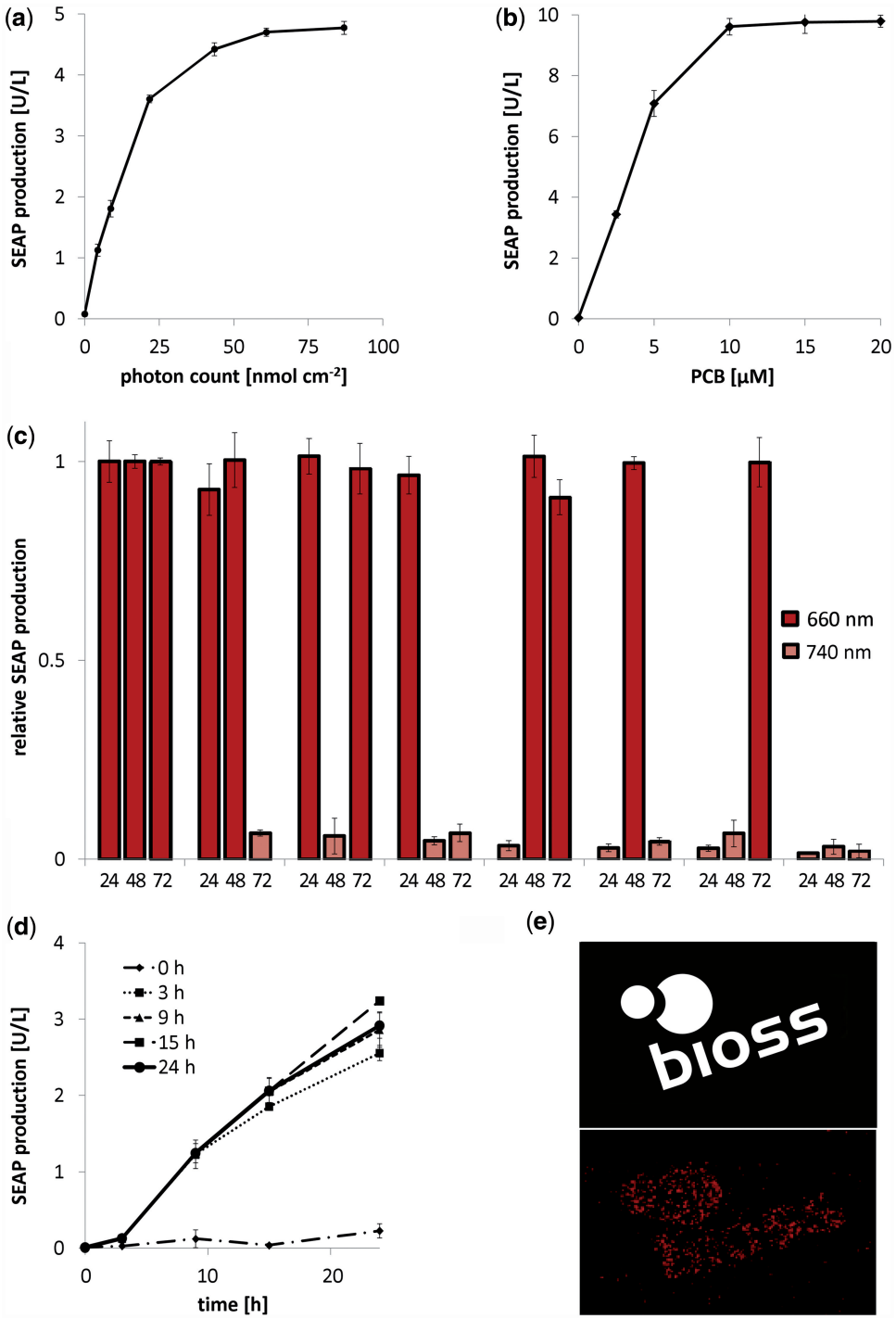

Figure 2. Detailed characterization of red light-inducible gene expression. (**a–d**) 70 000 CHO-K1 cells were transfected with the red light-inducible SEAP expression system (plasmids pKM006 and pKM022). After 24 h, the medium was replaced by fresh medium containing PCB (15 µM unless stated otherwise). The cells were cultivated for 1 h in the dark and subsequently subjected to the indicated illumination conditions before quantification of SEAP production. (a) Dose–response curve for red light-inducible SEAP expression. Cells were exposed to a 25 min pulse of 660 nm light at different intensities, resulting in the indicated photon number. After 24 h incubation in the dark, SEAP production was quantified. (b) PCB-adjustable transgene expression levels. Cells were exposed to a 25 min pulse of 660 nm light, resulting in a photon number of 80 nmol cm^{-2} for full induction of gene expression in the presence of increasing PCB concentrations. Subsequently, the cells were cultivated in the dark for 24 h before the quantification of SEAP production. (c) Reversibility of red light-inducible gene expression. Every 24 h, the cell culture medium was replaced by fresh PCB-containing medium, and the cells were illuminated at the indicated wavelengths. SEAP production was measured every 24 h. To correct for changes in gene expression over time because of cell growth, expression levels were normalized to the configuration, where cells were constantly kept under 660 nm light. (d) Effect of dark reversion of the PhyB–PIF6 interaction on transgene expression. Cells were grown under 660 nm light for the indicated periods before moving the cells to the dark. At the indicated time points, SEAP production was quantified. (**e**) Spatially resolved control of gene expression. CHO-K1 cells transgenic for red light-inducible mCherry expression (plasmids pKM022 and pKM078) were illuminated through a photo mask (top image) for 1 h (0.5 µmol m^{-2} s^{-1}). After 23 h incubation in the dark, mCherry production was visualized. Scale bar, 1 cm. In Figure 2a–d, data represent the mean of four independent experiments, and error bars indicate the standard deviations.

PCB–PhyB–VP16 complex (PPV) and the light condition. The light-dependent activation of the mRNA transcription is modeled by Monod kinetics. The production is activated by PPV with the maximal transcription rate k_{tc}. PPV can either be ON ($k_{light} = 1$) or OFF ($k_{light} = 0$). A switch between these two states can be triggered by light. The PPV complex is formed by PCB and PhyB–VP16. This is described with Michaelis–Menten enzyme kinetics with $v_{max} = k_{form,PPV}[PhyB{-}VP16]$ [Equation (2)]. The red light-dependent transcription factor PhyB–VP16 is produced by pKM022 with a constant rate. By using steady state assumptions, we can replace $[PhyB{-}VP16]$ with $\left(PhyB{-}VP16_{total_0} - [PPV]\right)$. All substances can decay with a half-life $T_{\frac{1}{2}} = \log(2)/k_{deg}$. We assumed exponential cell growth with the rate k_{growth}. The plasmids used are transfected transiently into the cells and are not replicated during cell division. Therefore, we introduced an equation for the gene dose of the transfected plasmids to describe the dilution caused by cell growth ($k_{dilution}$ equals the growth rate k_{growth}).

The output on protein level is SEAP or human $VEGF_{121}$ (VEGF). The dynamics of the protein concentration [VEGF] show a time delay to the corresponding dynamics of the mRNA concentration. To take this effect into account, we modeled the protein synthesis in two steps:

$$\text{mRNA} \rightarrow \text{Protein}_{\text{PRE}} \rightarrow \text{Protein}$$

where $\text{Protein}_{\text{PRE}}$ (P_{pre}) is the pre-protein subsequently being post-translationally modified and secreted.

To parameterize the model, we first determined the decay rates of intracellular PhyB–VP16 conjugated to PCB (Supplementary Figure S3a) and of free PCB in cell culture medium (Supplementary Figure S3b and d) by bioassay and absorbance measurement. For parameterizing the light-dependent shut-on and shut-off, we incubated CHO-K1 cells engineered for light-inducible VEGF production (plasmids pKM022 and pKM033) for 1 h in the presence of PCB before inducing expression by illumination at 660 nm (Figure 3a and b). After 6 h, cells were switched to 740 nm light, supplemented with tetracycline (to prevent binding of the transactivator to the promoter) or retained under 660 nm illumination. Gene expression was followed for the whole experiment by quantifying VEGF-specific mRNA (Figure 3a) and secreted VEGF protein (Figure 3b).

These data in combination with literature data (see Supplementary Information) were used to parameterize the model in Equation (1–8) by performing a multi-experiment fit (based on the data shown in Figure 3a and b and Supplementary Figure S3a and c) (Supplementary Table S2). The shaded error bands represent the error estimated by an error model (Supplementary Information) with a constant error σ_0 and a relative error σ_{rel}:

$$\sigma^2_{total}([conc]) = \sigma^2_0 + \sigma^2_{rel}[conc] \quad (9)$$

We applied this model to gain insight into the kinetics of light-regulated gene expression kinetics. For this aim, we calculated the mRNA production rate as a function of time and illumination conditions (Figure 3c). It can be seen that gene expression immediately rises after switching to 660 nm light ($t = 0$), whereas a transition to 740 nm ($t = 6$ h) induces an abrupt shut down of the target promoter activity. On continuous exposure to 660 nm light, the mRNA production rate decays, which can be explained by the limited stability of PCB in the cell culture environment. These rapid on and off kinetics make this system a highly useful tool for the reversible control of transgene activity.

To harness the precisely adjustable expression characteristics of the red light-inducible expression system for tissue engineering, we adapted the system to control neovascularization and angiogenesis. For this aim, expression of the human vascular endothelial growth factor splice variant 121 ($hVEGF_{121}$) was placed under red light control in CHO-K1 cells. The cells were subsequently embedded into a biocompatible, tissue-engineering-validated PEG-based hydrogel (18) and applied onto the CAM of chicken embryos at embryonic day 9 (24). The embryos were illuminated with 660 or 740 nm light for 48 h before analyzing the microvasculature (Figure 4). Although illumination at 740 nm resulted in a vascularization pattern corresponding to the negative control (Figure 4b and Supplementary Figures S4 and S5b, Supplementary Video Files), illumination at 660 nm showed strong signs of $hVEGF_{121}$-induced neovascularization and angiogenesis as indicated by a denser capillary plexus and typical brush- or delta-like ramifications and tortuous vascular structures (Figure 4a).

The first red/far-red light-switchable bi-stable mammalian gene expression system described here meets all criteria of an optimal inducible expression system (1): it has a low background expression, whereas it shows high expression levels that are rapidly and reversibly induced. Red light as the inducer enables spatial resolution of gene expression and is non-toxic. Moreover, the proteins used are orthogonal to mammalian cells and are, therefore, expected to minimally interfere with the endogenous metabolism. The genetic design of the system is compact, consisting of only two plasmids. Compared with previously described systems that use endogenous chromophores (2–4), handling of the phytochrome-based system is simpler, as protection from light is not required until the addition of the chromophore PCB. The chromophore is a non-toxic side effect-free natural compound used as food additive.

The two stable states, PhyB_{R} and PhyB_{FR}, confer toggle-like switching characteristics to this expression system. Although short pulses of 660 or 740 nm light are sufficient to induce or shut off gene expression, the system maintains its expression state in the dark, thus avoiding the need for prolonged illumination while still having the option to rapidly interfere with gene expression at any time point. These bi-stable–like, but still rapidly switchable, characteristics represent an advantage over previously described blue light-inducible expression systems, where reversion of gene expression was dependent on the spontaneous decay of transcription activation complexes (2,3) occurring with half-lives of several hours.

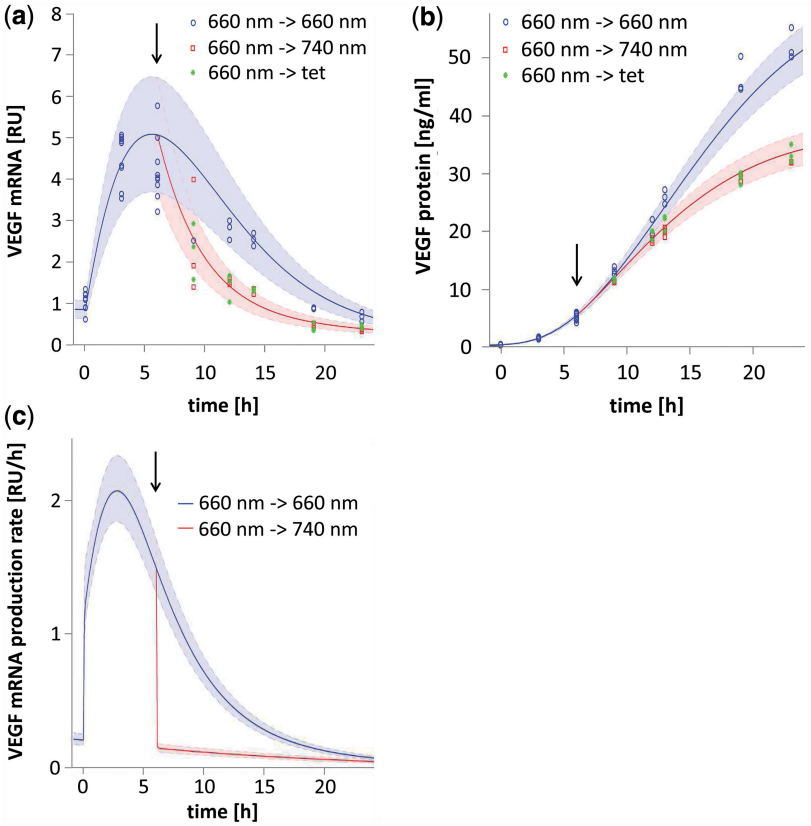

Figure 3. Model-based analysis of the light-responsive gene expression kinetics. In all, 70 000 CHO-K1 cells were transfected for red-light inducible $hVEGF_{121}$ expression (plasmids pKM022 and pKM033). After 24 h, the medium was supplemented with 15 μM PCB ($t = -1$ h). Cells were subsequently illuminated for 6 h at 660 nm and were then either switched to 660 nm, 740 nm or tetracycline-containing medium (arrow). (**a**) Switch-off kinetics of $hVEGF_{121}$ mRNA. At the indicated points in time, cells were lysed, and $hVEGF_{121}$ mRNA was quantified. (**b**) Switch-off kinetics of $hVEGF_{121}$ protein production. At the indicated points in time, $hVEGF_{121}$ was quantified in the cell culture supernatant. (**c**) Model prediction for the *de novo* synthesis of $hVEGF_{121}$ mRNA. In (a) and (b), the shaded error bands are based on the error model detailed in Equation (9). The shaded bands in (c) indicate the 95% prediction confidence interval, which was calculated by propagating the uncertainties of the estimated parameters.

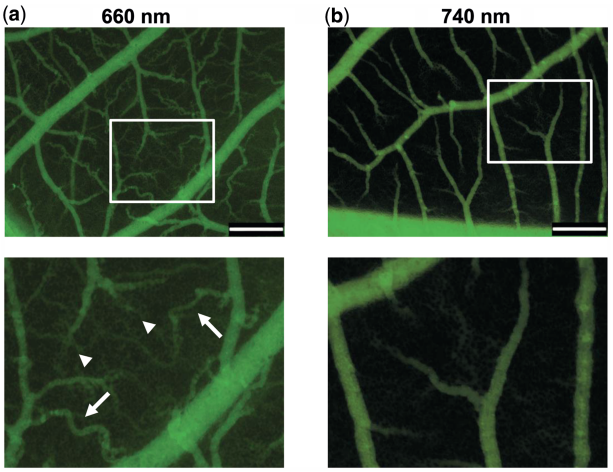

Figure 4. *In vivo* red light-controlled vascularization in chicken embryos. CHO-K1 cells were engineered for red light-inducible expression of the 121 amino acid splice variant of human vascular endothelial growth factor $hVEGF_{121}$. One million cells were embedded in 3% polyethylene glycol gel and were applied onto the CAM of 9 days old chicken embryos. After illumination at (**a**) 660 or (**b**) 740 nm for 48 h, the microvasculature was visualized by injection of FITC–dextran and video imaging (see Supplementary Material for videos). Brush- and delta-like endpoint patterns (arrowheads) and tortuously shaped vascularization (arrows) are indicated. Top panels, overview; lower panels, insets at higher magnification. Scale bar, 500 μm.

We anticipate that the rapidly reversible, tunable, space- and time-resolved expression characteristics of our red light-inducible expression system will become valuable for synthetic biological approaches in mammalian cells and will accelerate the progression of synthetic biology from fundamental research towards biomedical applications.

SUPPLEMENTARY DATA

Supplementary Data are available at NAR Online: Supplementary Information, Supplementary Tables 1–2, Supplementary Figures 1–5 and Supplementary Videos 1–2.

FUNDING

'Internationale Spitzenforschung II' of the Baden-Württemberg Stiftung [P-LS-SPII/2]; European Research Council under the European Community's Seventh Framework Programme [FP7/2007-2013]/ERC [259043]-CompBioMat; Excellence Initiative of the German Federal and State Governments [EXC 294]. Funding for open access charge: 'Internationale Spitzenforschung II' of the Baden-Württemberg Stiftung [P-LS-SPII/2].

Conflict of interest statement. A patent application has been filed by the Baden-Württemberg Stiftung covering this technology, for which K.M., M.M.K., M.D.Z., F.N. and W.W. are inventors.

REFERENCES

1. Weber,W. and Fussenegger,M. (2012) Emerging biomedical applications of synthetic biology. *Nat. Rev. Genet.*, **13**, 21–35.
2. Wang,X., Chen,X. and Yang,Y. (2012) Spatiotemporal control of gene expression by a light-switchable transgene system. *Nat. Methods*, **9**, 266–269.
3. Yazawa,M., Sadaghiani,A.M., Hsueh,B. and Dolmetsch,R.E. (2009) Induction of protein-protein interactions in live cells using light. *Nat. Biotechnol.*, **27**, 941–945.
4. Ye,H.F., Daoud-El Baba,M., Peng,R.W. and Fussenegger,M. (2011) A synthetic optogenetic transcription device enhances blood-glucose homeostasis in mice. *Science*, **332**, 1565–1568.
5. Khanna,R., Huq,E., Kikis,E.A., Al-Sady,B., Lanzatella,C. and Quail,P.H. (2004) A novel molecular recognition motif necessary for targeting photoactivated phytochrome signaling to specific basic helix-loop-helix transcription factors. *Plant Cell*, **16**, 3033–3044.
6. Shimizu-Sato,S., Huq,E., Tepperman,J.M. and Quail,P.H. (2002) A light-switchable gene promoter system. *Nat. Biotechnol.*, **20**, 1041–1044.
7. Tyszkiewicz,A.B. and Muir,T.W. (2008) Activation of protein splicing with light in yeast. *Nat. Methods*, **5**, 303–305.
8. Leung,D.W., Otomo,C., Chory,J. and Rosen,M.K. (2008) Genetically encoded photoswitching of actin assembly through the Cdc42-WASP-Arp2/3 complex pathway. *Proc. Natl. Acad. Sci. USA*, **105**, 12797–12802.
9. Levskaya,A., Weiner,O.D., Lim,W.A. and Voigt,C.A. (2009) Spatiotemporal control of cell signalling using a light-switchable protein interaction. *Nature*, **461**, 997–1001.
10. Fussenegger,M., Mazur,X. and Bailey,J.E. (1997) A novel cytostatic process enhances the productivity of Chinese hamster ovary cells. *Biotechnol. Bioeng.*, **55**, 927–939.
11. Fussenegger,M., Moser,S., Mazur,X. and Bailey,J.E. (1997) Autoregulated multicistronic expression vectors provide one-step cloning of regulated product gene expression in mammalian cells. *Biotechnol. Prog.*, **13**, 733–740.
12. Weber,W., Fux,C., Daoud-el Baba,M., Keller,B., Weber,C.C., Kramer,B.P., Heinzen,C., Aubel,D., Bailey,J.E. and Fussenegger,M. (2002) Macrolide-based transgene control in mammalian cells and mice. *Nat. Biotechnol.*, **20**, 901–907.
13. Weber,W., Stelling,J., Rimann,M., Keller,B., Daoud-El Baba,M., Weber,C.C., Aubel,D. and Fussenegger,M. (2007) A synthetic time-delay circuit in mammalian cells and mice. *Proc. Natl. Acad. Sci. USA*, **104**, 2643–2648.
14. Kunkel,T., Tomizawa,K., Kern,R., Furuya,M., Chua,N.H. and Schafer,E. (1993) In vitro formation of a photoreversible adduct of phycocyanobilin and tobacco apophytochrome B. *Eur. J. Biochem.*, **215**, 587–594.
15. Eriksen,N.T. (2008) Production of phycocyanin—a pigment with applications in biology, biotechnology, foods and medicine. *Appl. Microbiol. Biotechnol.*, **80**, 1–14.
16. Oliveira,E.G., Rosa,G.S., Moraes,M.A. and Pinto,L.A.A. (2008) Phycocyanin content of *Spirulina platensis* dried in spouted bed and thin layer. *J. Food Process Eng.*, **31**, 34–50.
17. Schlatter,S., Rimann,M., Kelm,J. and Fussenegger,M. (2002) SAMY, a novel mammalian reporter gene derived from *Bacillus stearothermophilus* alpha-amylase. *Gene*, **282**, 19–31.
18. Ehrbar,M., Rizzi,S.C., Hlushchuk,R., Djonov,V., Zisch,A.H., Hubbell,J.A., Weber,F.E. and Lutolf,M.P. (2007) Enzymatic formation of modular cell-instructive fibrin analogs for tissue engineering. *Biomaterials*, **28**, 3856–3866.
19. Djonov,V., Schmid,M., Tschanz,S.A. and Burri,P.H. (2000) Intussusceptive angiogenesis: its role in embryonic vascular network formation. *Circ. Res.*, **86**, 286–292.
20. Gossen,M. and Bujard,H. (1992) Tight control of gene expression in mammalian cells by tetracycline-responsive promoters. *Proc. Natl. Acad. Sci. USA*, **89**, 5547–5551.
21. Bacchus,W. and Fussenegger,M. (2012) The use of light for engineered control and reprogramming of cellular functions. *Curr. Opin. Biotechnol.*, **23**, 695–702.
22. Rockwell,N.C., Su,Y.S. and Lagarias,J.C. (2006) Phytochrome structure and signaling mechanisms. *Annu. Rev. Plant Biol.*, **57**, 837–858.
23. Kramer,B.P., Viretta,A.U., Daoud-El-Baba,M., Aubel,D., Weber,W. and Fussenegger,M. (2004) An engineered epigenetic transgene switch in mammalian cells. *Nat. Biotechnol.*, **22**, 867–870.
24. Ehrbar,M., Djonov,V.G., Schnell,C., Tschanz,S.A., Martiny-Baron,G., Schenk,U., Wood,J., Burri,P.H., Hubbell,J.A. and Zisch,A.H. (2004) Cell-demanded liberation of VEGF121 from fibrin implants induces local and controlled blood vessel growth. *Circ. Res.*, **94**, 1124–1132.